

Published in final edited form as:

*Proc SPIE*. 2007 January 1; 6510: . doi:10.1117/12.710109.

## Photon-counting gamma camera based on columnar CsI(Tl) optically coupled to a back-illuminated CCD

Brian W. Miller<sup>a</sup>, H. Bradford Barber<sup>a</sup>, Harrison H. Barrett<sup>a</sup>, Liying Chen<sup>a</sup>, and Sean J. Taylor<sup>b</sup>

<sup>a</sup> College of Optical Sciences and Department of Radiology, University of Arizona, Tucson, AZ 85721

<sup>b</sup> Lockheed Martin Space Systems, Sunnyvale, CA 94089

### Abstract

Recent advances have been made in a new class of CCD-based, single-photon-counting gamma-ray detectors which offer sub-100  $\mu\text{m}$  intrinsic resolutions.<sup>1-7</sup> These detectors show great promise in small-animal SPECT and molecular imaging and exist in a variety of configurations. Typically, a columnar CsI(Tl) scintillator or a radiography screen ( $\text{Gd}_2\text{O}_2\text{S:Tb}$ ) is imaged onto the CCD. Gamma-ray interactions are seen as clusters of signal spread over multiple pixels. When the detector is operated in a charge-integration mode, signal spread across pixels results in spatial-resolution degradation. However, if the detector is operated in photon-counting mode, the gamma-ray interaction position can be estimated using either Anger (centroid) estimation or maximum-likelihood position estimation resulting in a substantial improvement in spatial resolution.<sup>2</sup> Due to the low-light-level nature of the scintillation process, CCD-based gamma cameras implement an amplification stage in the CCD via electron multiplying (EMCCDs)<sup>8-10</sup> or via an image intensifier prior to the optical path.<sup>1</sup>

We have applied ideas and techniques from previous systems to our high-resolution LumiSPECT detector.<sup>11, 12</sup> LumiSPECT is a dual-modality optical/SPECT small-animal imaging system which was originally designed to operate in charge-integration mode. It employs a cryogenically cooled, high-quantum-efficiency, back-illuminated large-format CCD and operates in single-photon-counting mode without any intermediate amplification process. Operating in photon-counting mode, the detector has an intrinsic spatial resolution of 64  $\mu\text{m}$  compared to 134  $\mu\text{m}$  in integrating mode.

### Keywords

Photon-Counting; EMCCD; molecular imaging; columnar CsI(Tl); SPECT; Bazooka SPECT detector

## 1. INTRODUCTION

Recent advances in CCD technology have brought about a new generation of high-resolution detectors for small-animal Single Photon Emission Computed Tomography (SPECT) and molecular imaging.<sup>1-7, 13</sup> Such detectors have intrinsic resolutions better than 100  $\mu\text{m}$  and employ scintillators such as columnar CsI(Tl)<sup>14</sup> or terbium-doped gadolinium oxysulfide ( $\text{Gd}_2\text{O}_2\text{S:Tb}$ ) phosphor screens. Gamma-ray interactions in columnar CsI(Tl) scintillators or in radiography screens are imaged onto a CCD as clusters of signal. These detectors operate

in photon-counting mode when individual interactions are seen as spatially separable events. This process occurs when the frame rate or acquisition time of the CCD is fast enough so that clusters do not overlap. Due to the low-light-level nature of the scintillation process, gain processes have been used to amplify the signal for single-photon detection. Electron-multiplying CCDs have been shown to function as gamma cameras by amplifying the signal prior to the charge-to-voltage conversion process.<sup>5-7</sup> Typically, a columnar CsI(Tl) scintillator is directly coupled to an EMCCD via a fiber optic window.<sup>2, 5, 7, 15</sup> A fiber optic taper can be used to increase active imaging area. It has also been shown that the use of an electrostatic demagnifier (DM) tube, a first-generation image intensifier, coupled to an EMCCD via a fiber optic taper can be used to provide an enlarged active imaging area.<sup>3</sup> Another detector, Bazooka SPECT, employs a second/third generation image intensifier where gain is applied prior to the optical path.<sup>1</sup> Amplification prior to the optical path negates light loss experienced by other systems allowing for great flexibility in the imaging system design. Bazooka SPECT's optical system consists of lenses in a macro-photography configuration where the output screen of the image intensifier is imaged onto a low-cost CCD. The optical system design for Bazooka SPECT stems from our LumiSPECT detector at the Center for Gamma-Ray Imaging.<sup>11, 12</sup>

LumiSPECT is a high-resolution dual-modality optical/SPECT small-animal imaging system, Taylor *et al.*<sup>11, 12</sup> It employs a cryogenically cooled, high-quantum-efficiency, back-illuminated large-format CCD whose properties are listed in Table 1. In optical mode, the detector is capable of imaging standard optical reporters such as luciferase, GFP, and RFP. For SPECT imaging, it was originally designed to operate in gamma-ray flux-integration mode using standard nuclear medicine radiotracers and the Gamma Converter,<sup>11, 12</sup> a parallel-hole collimator coupled to a columnar CsI(Tl) scintillator.

We have applied ideas and techniques from the previously mentioned gamma cameras to operate LumiSPECT in single-photon-counting mode without any intermediate amplification process. Operating the LumiSPECT system in photon-counting mode has yielded a significant improvement in spatial resolution.

## 2. INSTRUMENTATION/METHODS

### 2.1. Optical System

The LumiSPECT optical system is the same as that used in macro photography, a type of close-up photography. In macro-photography configuration, a standard camera lens is attached to the CCD and a second lens is mounted in a reversed position. With both lenses focused at infinity, an object placed at the front focal plane of the reversed lens, a distance of 46.5 mm from the flange of a Nikon F-mount lens, will be imaged onto the CCD with magnification of the object given by the ratio of the focal lengths:

$$\text{magnification} = \frac{f_1}{f_2}. \quad (1)$$

Macro-photography configuration has several attractive features. First, this optical configuration can offer high-light collection efficiency. For photon counting, we operate the detector in a 1:1 imaging configuration using two 50 mm F/1.2 Nikon Nikkor lenses as shown in Figure 1. Another advantage of macro configuration is that customizable magnification is easily obtained. For example, a 400 mm focal length lens coupled to a reversed 50 mm lens will result in a magnification of 8×. In this configuration, we can examine the columnar CsI(Tl) crystal at high magnification. Scintillation effects in columnar CsI(Tl) due to fiber diameter and scintillator thickness are not fully understood and are currently under investigation. Flood illuminating the columnar CsI(Tl) crystal with an x-ray or gamma-ray source and examining

it at high magnification may aid in detecting crystal defects and in better understanding the scintillation process in columnar CsI(Tl) crystallites.

## 2.2. Photon Counting

Gamma-ray/scintillator interactions appear as clusters of signal spread over multiple pixels as seen in Figure 2a. To improve the detector spatial resolution, individual gamma-ray clusters are extracted, and an Anger (centroid) calculation is used to estimate the interaction position to much better than the spread of the light distribution as shown in Figure 2b. To extract clusters, we implement similar techniques as those used in image-intensified (Bazooka SPECT) and EMCCD gamma cameras.<sup>1, 6, 7, 9</sup> First, a background image is subtracted and then the frame is thresholded slightly above the noise variance. Next, each frame is searched for contiguous regions of signal above the threshold, which are then identified as individual events. A centroid calculation is then performed on a window (e.g.,  $9 \times 9$ ) around each identified event. The centroid calculation can also be used for subpixel position estimation and has been shown to yield additional improvement in spatial resolution.<sup>1, 2</sup> Other techniques employ maximum-likelihood (ML) estimation to estimate the 3D position and energy of individual gamma-ray interactions and can be used to correct for depth-of-interaction effects.<sup>2</sup> Application of maximum-likelihood techniques to the LumiSPECT system is currently under investigation.

The LumiSPECT CCD has a full-frame readout of 36 seconds at 50 kHz and 1.8 seconds at 1 MHz. To reduce frame readout time, a combination of CCD binning, region of interest (ROI) selection, and/or selection of a faster readout rate is used. Photon-counting mode functions best at 50 kHz but is also possible at 1 MHz with higher energy isotopes such as Tc99m.

## 3. RESULTS

### 3.1. Spatial Resolution

Operating the LumiSPECT detector in photon-counting mode, we are able to estimate the interaction position to better than the spread of the light distribution. To measure the intrinsic resolution of the detector, a 1 cm thick slab of tungsten with a  $25 \mu\text{m}$  slit opening was placed on a  $270 \mu\text{m}$  thick RMD columnar CsI(Tl) scintillator. The detector was illuminated with a point source of 120 keV,  $\text{Co}^{57}$  gamma rays. In the gamma-ray/scintillator interaction, optical photons were generated and sampled over multiple pixels. Individual gamma-ray interactions were obtained with the camera operating in photon-counting mode. Two-thousand frames were collected and binned at  $1 \times 1$  to sample at  $20 \times 20 \mu\text{m}^2$  pixels with an integration time of 0.5-seconds per frame. In addition, a 1000 second integrated image was collected for a resolution comparison of LumiSPECT operating in photon/integration modes. Slit images are shown in Figure 3a–b.

To evaluate the spatial resolution improvement using centroid estimation, MTFs and LSFs were generated for photon-counting and integration modes and are shown in Figure 3c,d. Results show significant improvement in spatial resolution using centroid estimation compared to operation in charge-integration mode. As shown from the Line Spread Function (LSF) in Figure 3-c, a spatial resolution of approximately  $64 \mu\text{m}$  (FWHM) is obtained using centroid estimation compared to  $134 \mu\text{m}$  (FWHM) for the integrated image. Such improvements are significant as studies have shown that small enhancements in spatial resolution can result in large improvements in objective performance measures.<sup>16</sup>

### 3.2. Resolution Phantom

To demonstrate the high-resolution capability of LumiSPECT in photon-counting mode, we created a phantom using ion-exchange beads with a total absorption of approximately 130  $\mu\text{Ci}$  of  $\text{Tc}^{99\text{m}}$ . The phantom consisted of six, approximately  $250 \mu\text{m}$  diameter beads. The

phantom was placed a distance of 4 mm from a 250  $\mu\text{m}$  pinhole, and the 270  $\mu\text{m}$  columnar CsI (Tl) screen was placed 31 mm from the pinhole. This imaging configuration resulted in a magnification of 7.75 $\times$  and yielded an estimated resolution of 280  $\mu\text{m}$ . Four thousand 0.5-second frames were acquired and individual gamma-ray interactions were estimated. A corresponding 2000-second Lu-miSPECT integrated image was acquired. White light, integration, and photon-counting images demonstrating the resolution capabilities are shown in Figure 4.

### 3.3. Energy Resolution

To test the energy resolution of the system, we used an RMD 270  $\mu\text{m}$  columnar CsI(Tl) scintillator and flood illuminated the detector with  $\text{Am}^{241}$ ,  $\text{Co}^{57}$ , and  $\text{Tc}^{99m}$  isotopes. Individual events were extracted and the total sum signal within a  $9 \times 9$  region was used to generate energy histograms, analogous to pulse-height spectra, shown in Figure 5. The mean signal (ADU units) in a  $9 \times 9$  region around clusters for  $\text{Am}^{241}$  is 378 units, 478 units for  $\text{Co}^{57}$ , and 523 units for  $\text{Tc}^{99m}$ , indicating that light output scales linearly with energy. However, we see a large variance in sum signal for a given isotope and the energy spectra in Figure 5 indicate that variance increases with isotope energy. Consequently, although this system is capable of photon counting, the low-light level imaging without amplification results in energy-discrimination difficulties compared to image-intensified and EMCCD gamma cameras.<sup>1, 2, 5, 6</sup> This poses difficulties for dual-isotope SPECT imaging in LumiSPECT, but for single-isotope imaging, energy resolution is less important in small-animal imaging compared with that required in clinical systems.<sup>12</sup>

## 4. FUTURE WORK

Photon counting in the LumiSPECT system allows for energy estimation of individual gamma-ray interactions. Light output from gamma-ray interactions varies as a function of depth; therefore, summing the signal within a cluster is not the optimal method for energy estimation. It was demonstrated by Miller *et al.* that the use of maximum-likelihood (ML) energy estimation in EMCCD photon-counting detectors yielded improvements in energy resolution.<sup>2</sup> For maximum-likelihood energy estimation in the EMCCD gamma camera, the mean signal was assumed to be a 2-D spatial gaussian whose variance and sum signal varied as a function of depth. When the depth-dependent, functional forms of light output and spatial variance were acquired, the likelihood and corresponding log-likelihood were generated. The likelihood and log-likelihood are functions of the data given the parameters to be estimated ( $x, y, z, E$ ). Finding the parameters which minimized the negative of log-likelihood yielded the maximum-likelihood 3-D ( $x, y, z$ ) position and energy ( $E$ ) estimates for individual gamma-ray interactions.

For LumiSPECT, we originally assumed that the mean signal could be described by a 2-D gaussian, however, we did not see an improvement in energy resolution. Upon closer examination of data, we have found that a 2-D spatial gaussian is not the proper model. Instead of a gaussian profile, we see individual clusters having negative kurtosis (flatter profile). In future work, we anticipate that application of a model which better describes the spatial profile of individual gamma-ray interactions will yield improvements in energy resolution.

## 5. CONCLUSION

We have demonstrated that the LumiSPECT system is capable of operating in photon-counting mode without any intermediate amplification process. Compared to other CCD-based gamma cameras,<sup>1, 2, 5, 6</sup> energy resolution tests show the detector to have poorer performance in energy discrimination. However, it is anticipated that improvements in energy resolution are possible with a model which describes the spatial profile of gamma-ray interactions and through the use maximum-likelihood techniques. Spatial resolution tests show LumiSPECT to have an

intrinsic spatial resolution comparable to other systems; an interesting result considering no intermediate amplification is implemented such as is required in EMCCD and image-intensifier-based gamma cameras. In photon-counting mode, LumiSPECT has an estimated intrinsic spatial resolution of  $64\ \mu\text{m}$  compared to  $134\ \mu\text{m}$  when operated in charge-integration mode. It is anticipated that the substantial improvements in spatial resolution of CCD-based gamma-ray detectors will be extremely utile in small-animal SPECT and molecular imaging.

## Acknowledgments

The Center for Gamma-Ray Imaging is supported by NIH Grant P41 EB 002035-8. The authors would like to thank Dr. Vivek V. Nagarkar of Radiation Monitoring Devices, Inc. (RMD) for the use of their columnar CsI(Tl) scintillators. The authors would also like to thank Charles (Pier) Ingram for assistance with image acquisition.

## References

1. Miller, BW.; Barber, HB.; Barrett, HH.; Wilson, DW.; Chen, L. A low-cost approach to high-resolution, single-photon imaging using columnar scintillators and image intensifiers. Presented at IEEE 2006 NSS/MIC; October 29-November 4, 2006;
2. Miller BW, Barber H, Barrett H, Shestakova I, Singh B, Nagarkar V. Single-photon spatial and energy resolution enhancement of a columnar CsI (Tl)/EMCCD gamma-camera using maximum-likelihood estimation. *Proc SPIE* 2006;6142:61421T.
3. Meng L. An Intensified EMCCD Camera for Low Energy Gamma Ray Imaging Applications. *Nuclear Science, IEEE Transaction* August;2006 53:2376–2384.
4. Nagarkar VV, Gaysinskiy V, Shestakova I, Singh B, Teo K, Sun M, Barber WC, Hasegawa B. Near simultaneous combined spect/ct imaging using emccd. *IEEE NSS/MIC Conf Rec* 2005;5:2607–2610.
5. Beekman F, de Vree G. Photon-counting versus an integrating CCD-based gamma camera: important consequences for spatial resolution. *Physics in Medicine and Biology* 2005;50(12):N109–N119. [PubMed: 15930598]
6. Teo K, Shestakova I, Sun M, Barber WC, Hasegawa BH, Nagarkar VV. Evaluation of a emccd detector for emission-transmission computed tomography. *IEEE NSS/MIC Conf Rec* 2005;5:3050–3054.
7. Nagarkar VV, Shestakova I, Gaysinskiy V, Singh B, Miller BW, Barber HB. Fast x-ray/ $\gamma$ -ray imaging using electron multiplying ccd-based detector. *Nuclear Instruments and Methods in Physics Research Section A: Accelerators, Spectrometers, Detectors and Associated Equipment* Jul 1;2006 563:45–48.
8. Denvir D, Conroy E. Electron multiplying CCDs. *Proceedings of SPIE* 2003;4877:55.
9. de Vree GA, van der Have F, Beekman FJ. Emccd-based photon-counting mini gamma camera with a spatial resolution  $< 100\ \mu\text{m}$ . *IEEE NSS/MIC Conf Rec* 2004;5:2724–2728.
10. Hyneczek J, Inc I, Allen T. Impactron-a new solid state image intensifier. *Electron Devices, IEEE Transactions* 2001;48(10):2238–2241.
11. Taylor, SJ. Master's thesis. University of Arizona, Department of Optical Sciences; Tucson, Arizona: 2004. Dual Modality Imaging With a Lens-Coupled CCD Camera.
12. Taylor, S.; Barrett, H.; Zinn, K. Small animal SPECT using a lens-coupled CCD camera. Poster presentation, Academy of Molecular Imaging; March, 2004;
13. Nagarkar VV, Singh B, Shestakova IK, Gaysinskiy V. Design and performance of an emccd based detector for combined spect/ct imaging. *IEEE NSS/MIC Conf Rec* 2005;4:2179–2182.
14. Miller, S.; Gaysinskiy, V.; Shestakova, I.; Nagarkar, V. Recent advances in columnar CsI (Tl) scintillator screens. In: James, Ralph B.; Franks, Larry A.; Burger, Arnold, editors. *Hard X-Ray and Gamma-Ray Detector Physics VII*; Proceedings of the SPIE; 2005. p. 99-108.
15. de Vree G, Westra A, Moody I, van der Have F, Ligtoet K, Beekman F. Photon-counting gamma camera based on an electron-multiplying CCD. *Nuclear Science, IEEE Transactions* 2005;52(3):580–588.
16. Barrett H. Objective assessment of image quality: effects of quantum noise and object variability. *J Opt Soc Am A* 1990;7(7):1266–1278. [PubMed: 2370589]

LumiSPECT Photon Counting Configuration



**Figure 1.** LumiSPECT imaging configuration. The optical system consists of two 50 mm Nikkor F/1.2 lens in a macrophotography configuration.

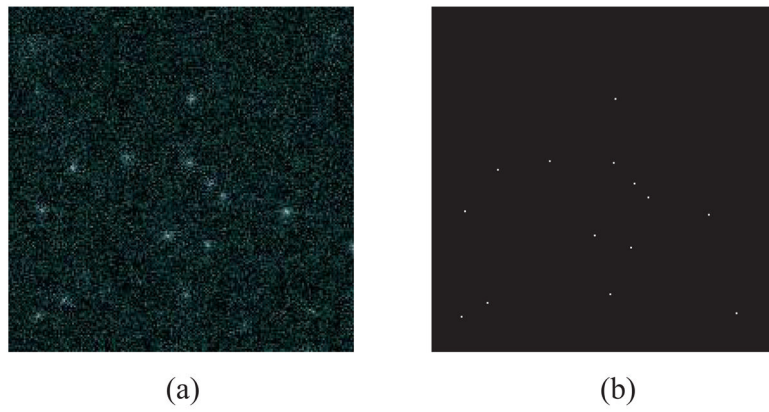


**Figure 2.**  
(a)  $\text{Tc}^{99m}$  140 keV gamma-ray interactions in columnar CsI(Tl) and (b) Anger (centroid) position estimations of gamma-ray interactions.

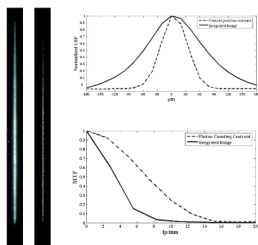


**Figure 3.** LumiSPECT resolution tests using a  $25 \mu\text{m}$  tungsten slit and an RMD  $270 \mu\text{m}$  columnar CsI (Tl) scintillator. The slit was illuminated with a 10 mCi  $\text{Co}^{57}$  point source. The data were binned at  $1 \times 1$  to sample at  $20 \times 20 \mu\text{m}^2$  pixels. (a) LumiSPECT slit in charge-integration mode with an acquisition time of 1,000 seconds, (b) photon-counting slit acquired with 2,000, 0.5-second frames, (c) Line Spread Function (LSF) for photon-counting (FWHM  $64 \mu\text{m}$ ) and charge-integration (FWHM  $134 \mu\text{m}$ ) slit images, and (d) Modulation Transfer Function (MTF) for photon-count and charge-integration slit images.



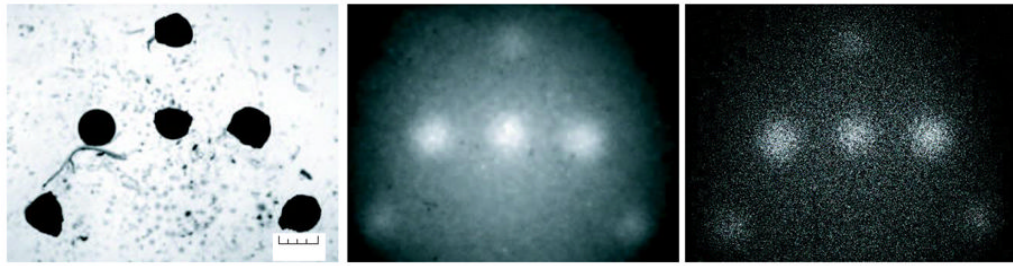


**Figure 4.** Resolution phantom using 250  $\mu\text{m}$  diameter  $\text{Tc}^{99\text{m}}$  ion-exchange beads: (a) white light microscope image, (b) LumiSPECT projection image in integration mode with an acquisition time of 2,000 seconds, (c) LumiSPECT photon-counting projection image using 4,000 frames with an integration time of 0.5-seconds per frame.

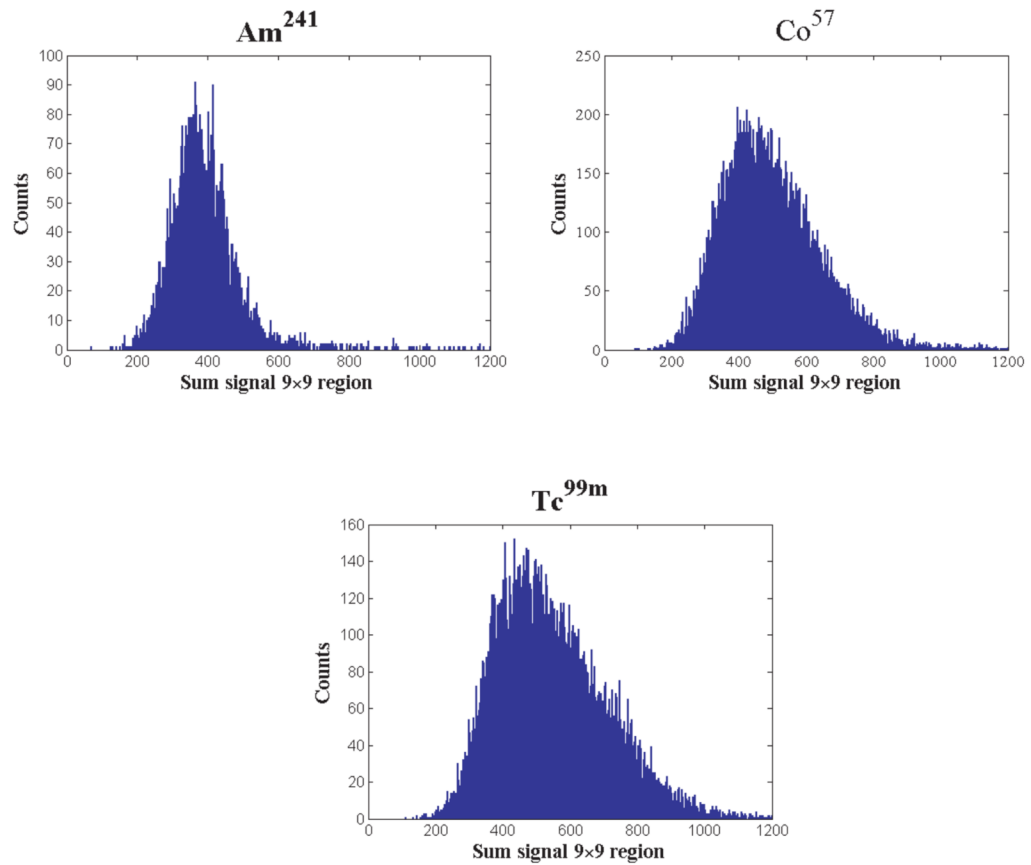


**Figure 5.** Energy spectra of an RMD 270  $\mu\text{m}$  thick columnar CsI(Tl) flood illuminated with (a)  $\text{Am}^{241}$ , (b)  $\text{Co}^{57}$ , (c) and  $\text{Tc}^{99\text{m}}$  isotopes. Histograms were generated using the sum signal within a  $9 \times 9$  region around each cluster.

**Table 1**LumiSPECT CCD Properties<sup>11, 12</sup>

Detector Type	VersArray 1300B, scientific grade
CCD Format	1340 × 1340 × 20 $\mu$ m pixels
Dark Current	0.1e <sup>-</sup> /pixel/sec@-40°C, 0.5e <sup>-</sup> /pixel/hr@-110°C
Read Noise	3e <sup>-</sup> @ 50 kHz scan rate, 12e <sup>-</sup> @ 1 MHz scan rate
Binning Modes	2 × 2, 3 × 3, 4 × 4
Full-frame Readout	36 sec @ 50 kHz, 1.8 sec @ 1MHz
Thermal Precision	±0.1°C over entire temperature range
Nonuniformity	≤ 4% over active area of CCD